



Classification of resonances and pairing effects on n - A scattering within the Hartree-Fock-Bogoliubov framework

K. Mizuyama ^{1,2}, H. Cong Quang,^{3,4} T. Dieu Thuy,³ and T. V. Nhan Hao ^{3,4,*}

¹*Institute of Research and Development, Duy Tan University, Da Nang 550000, Vietnam*

²*Faculty of Natural Sciences, Duy Tan University, Da Nang 550000, Vietnam*

³*Faculty of Physics, University of Education, Hue University, 34 Le Loi Street, Hue City, Vietnam*

⁴*Center for Theoretical and Computational Physics, University of Education, Hue University, 34 Le Loi Street, Hue City, Vietnam*



(Received 8 March 2021; revised 17 May 2021; accepted 23 August 2021; published 7 September 2021)

The properties of the scattering solutions obtained as poles of the S and K matrices are analyzed in terms of pairing effects in the framework of the Hartree-Fock-Bogoliubov (HFB) Jost function. As a result of our analysis, we found the following: in order for the poles of the S matrix to form a resonance, there must be a pole of the K matrix nearby. Within the framework of HFB theory, there are three types of resonance states; shape resonances, particle-type, and hole-type quasiparticle resonances. Other scattering states that can be classified are independent K - and S -matrix poles. It is shown both numerically and qualitatively using the Jost function that the pair-correlation effect is hardly observed in the shape resonance state, and that the appearance of the pair-correlation effect is different in the particle-type and hole-type quasiparticle resonance. We also found a noteworthy correlation effect that independent K -matrix poles break the metastable structure of the wave function of the quasiparticle resonance and turn it into an independent S -matrix pole. The correlation effect that the poles of the independent S matrix break the metastable structure of the inner wave function without breaking the resonance structure of the outer wave function when a pole of the independent S matrix is near the hole-type resonance state was also revealed. This is considered to be another aspect of the Fano effect.

DOI: [10.1103/PhysRevC.104.034606](https://doi.org/10.1103/PhysRevC.104.034606)

I. INTRODUCTION

Many sharp resonance peaks at the low-energy region of the neutron elastic cross section is one of the most important characteristics of nuclei. Those peaks have been analyzed by the resonance formula derived from the R -matrix theory [1]. Resonance parameters have been used for the wide purposes, such as the nuclear power technology, radiation therapy, and so on. However, it is difficult to understand the physics of resonance from the resonance parameters because the R -matrix theory is a phenomenological theory, there is no clear interpretation of physics for each parameter. In addition, there are several types of the resonance formula, which has the different interpretation in physics [2,3], although all of those are consistent with the Feshbach projection theory [4]. As a consequence of the R -matrix and Feshbach projection theory, the coupling of channels has the crucial role of the production of the sharp resonance peaks. Recently, the continuum particle-vibration coupling method succeeded to reproduce some of the sharp resonances, and it was shown that those peaks originate from the coupling between an incoming neutron and the collective excitation (especially the giant resonances) of target nucleus [5].

The Jost function [6] may be the appropriate method to understand the physics of the resonance because the Jost

function is calculated by the wave function and potential to represent the appropriate boundary condition for a regular solution of the Schrodinger equation so as to connect the regular and irregular solutions, and the zeros of the Jost function on the complex energy plane represent the poles of the S matrix corresponding to the bound states and resonances. However, the single channel has been supposed in the original Jost function. The extension of the Jost function is necessary so as to take into account the channels coupling. As a first step of the extension of the Jost function, we have extended the Jost function within the HFB formalism [7]. In a broad sense, the HFB formalism is also the channel coupling formalism for two channels, because the pairing correlation causes the mixing of the particle and hole configurations.

The pairing correlation is one of the most important correlations to describe not only the fundamental properties but also the many varieties of interesting phenomena of open-shell nuclei. The roles of the pairing correlation have been discussed for a long time on the ground state and excited states of open-shell nuclei. The important roles of pairing correlation for the exotic structure and dynamics of the neutron-rich nuclei were also revealed such as the two-neutron halo [8,9], dineutron [10], antihalo effect [11–13], pair rotation [14], and so on, in the last decades. Observation of those phenomena by nuclear reaction is one of the most important issues. The importance of the pairing correlation in the two-neutron transfer reaction has been discussed [15]. Very recently, it was shown that the quasiparticle resonance may be possible to be found as

*Corresponding author: tvnhao@hueuni.edu.vn

a sharp peak of the neutron elastic scattering cross section off the open-shell nucleus within the Hartree-Fock-Bogoliubov (HFB) theory [7,16].

In Figs. 9 and 11 of Ref. [7], we have shown the trajectories of the S -matrix poles to show the dependence on the mean value of the pairing for the stable and neutron-rich unstable nuclei. The S -matrix poles have been classified into two types; the hole-type and particle-type poles of quasiparticle resonances. The quasiparticle resonance originates from the Hartree-Fock (HF) single-particle or hole state due to the particle and hole configuration mixing by the pairing correlation. The pairing effect on the hole-type resonance and the interference effect with continuum have been discussed in terms of the Fano effect [17].

The shape resonance [18] is one of the well-known types of resonance. As is written in many textbooks of quantum physics, a shape resonance is a metastable state in which a nucleon is trapped due to the shape of the centrifugal barrier of the mean-field potential of the target nucleus. The wave function of the internal region is connected to the one of the external region through the tunneling effect. The shape resonance is not affected by the occupation of the nucleons in the potential (i.e., no dependence on the Fermi energy). The overall shape of the neutron elastic cross section is mainly determined by those shape resonances.

At first, we thought all of S -matrix poles that are found within the HFB framework can be classified in particle-type or hole-type. However, in Ref. [7], we noticed that some poles ($d_{5/2}$ for example) have different types of the dependence on the pairing from neither particle-type nor hole-type poles. This may imply that we need further classification for the S -matrix poles. In this paper, we will, therefore, try to classify the S -matrix poles and discuss the pairing dependence on each type of pole.

II. ANALYSIS

In the scattering system of the physics, there are three kinds of quantities, the S , T , and K matrix [19,20]. As is well known, the S matrix is the unitary matrix, which connects asymptotically sets of the free particle states in the Hilbert space of the physical states, such as the bound states, virtual states, and resonances. The physical states are represented as the poles of the S matrix on the complex energy plane. The T matrix is a quantity, which is directly connected with the cross section. The K matrix is defined as the Hermite matrix. All of those quantities are related to each other, and it has been believed that all of those quantities have the same information but different mathematical properties.

As is known, the S -matrix pole exhibits the bound state, virtual state, and resonance depending on the position on the complex energy/momentum plane. The bound and virtual states are the states that exist on the real axis of the first and second Riemann sheets of the complex energy, respectively. The resonance is the S -matrix pole, which exists on the second Riemann sheet. The real and imaginary part of a pole represent the resonance energy and width [21]. There is another definition of the resonance. In Ref. [22], the resonance has been defined by the Sturm-Liouville eigenvalues. It is possible

to show that the Sturm-Liouville eigenvalues are equivalent with the poles of the K matrix as shown in Appendix A. Note that the width of the resonance is defined by the resonance formula, which is derived in Ref. [22].

However, it is clear that the S matrix and K matrix have the different mathematical properties, and also their poles have the different properties and physical meaning. By using the Jost function, the difference in mathematical properties between the S and K matrices can be made more clear. The S matrix is defined as the ratio of the determinant of the Jost function to its complex conjugate. The K matrix is defined as the ratio of the real and imaginary parts of the determinant of the Jost function. The S -matrix poles are given by zeros of the determinant of the Jost function, and the K -matrix poles are given by zeros of the real part of the determinant of the Jost function. The Jost function is defined as a function connecting regular and irregular solutions, and the S matrix defined by the Jost function provides the proper scattering boundary condition in the scattering state. The poles of the K matrix appearing on the real axis of the complex energy also provide the boundary condition for the standing wave solution.

A. S and K matrix and scattering states of n - A scattering without pairing

Within the HF framework, the S matrix is expressed as

$$S_{lj}^{(0)}(\epsilon) \equiv \frac{J_{0,lj}^{(-)}(\epsilon)}{J_{0,lj}^{(+)}(\epsilon)}, \quad (1)$$

since single-channel system is supposed in the HF framework, and the S -matrix pole ϵ_R^0 is given by

$$J_{0,lj}^{(+)}(\epsilon_R^0) = 0, \quad (2)$$

where $J_{0,lj}^{(\pm)}(\epsilon)$ is the HF Jost function.

The K matrix can be expressed by using the Jost function as

$$K_{lj}^{(0)}(\epsilon) = i \left(\frac{J_{0,lj}^{(-)}(\epsilon) - J_{0,lj}^{(+)}(\epsilon)}{J_{0,lj}^{(-)}(\epsilon) + J_{0,lj}^{(+)}(\epsilon)} \right) \quad (3)$$

and the pole of the K matrix is given by

$$J_{0,lj}^{(+)}(\epsilon_n^0) + J_{0,lj}^{(-)}(\epsilon_n^0) = 0. \quad (4)$$

Since the scattering wave function $\psi_{0,lj}^{(+)}(r; \epsilon)$ is expressed as

$$\psi_{0,lj}^{(+)}(r; \epsilon) = \frac{1}{2}(v_{lj}^{(-)}(r; \epsilon) + S_{lj}^{(0)}(\epsilon)v_{lj}^{(+)}(r; \epsilon)), \quad (5)$$

$\psi_{0,lj}^{(+)}(r; \epsilon)$ becomes

$$\psi_{0,lj}^{(+)}(r; \epsilon_n^0) = \frac{1}{2}(v_{lj}^{(-)}(r; \epsilon_n^0) - v_{lj}^{(+)}(r; \epsilon_n^0)), \quad (6)$$

at $\epsilon = \epsilon_n^0$. This is a solution of Eq. (A12), which has a typical behavior of the standing wave solution because $v_{lj}^{(\pm)}$ has the asymptotic behavior of the outgoing/incoming wave.

Obviously, the S -matrix and K -matrix poles are independent because Eqs. (2) and (4) are independent. When the S -matrix pole is found, the K -matrix pole is not guaranteed to be found. The total neutron elastic cross section, which is

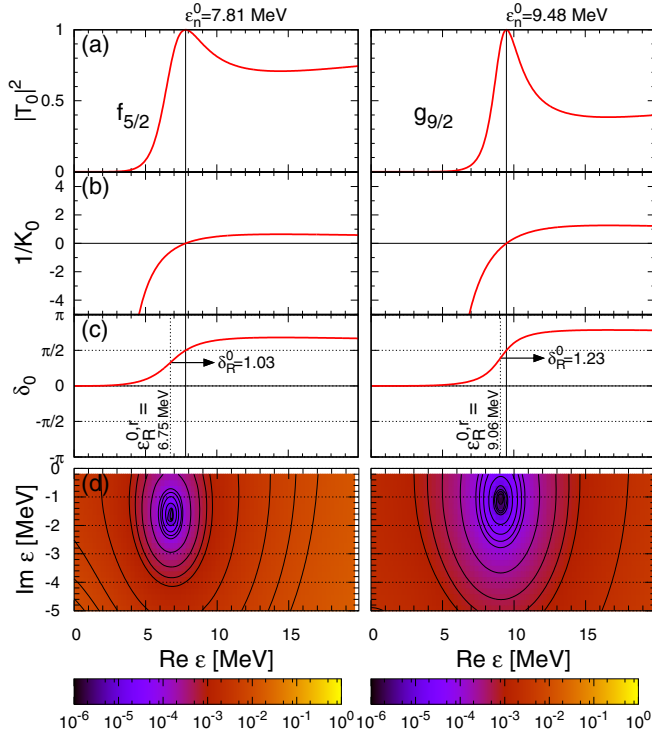


FIG. 1. The numerical results for $f_{5/2}$ and $g_{9/2}$ of square of T matrix $|T_{lj}^{(0)}|^2$, the inverse of the K matrix $1/K_{lj}^{(0)}$, and the phase shift δ_0 determined $S_{lj}^{(0)} = e^{2i\delta_0}$ are plotted as a function of the incident neutron energy ϵ in (a)–(c), respectively. In (d), the square of the Jost function $|J_{0,lj}^{(+)}(\epsilon)|^2$ is shown on the complex- ϵ plane.

shown in Ref. [7] consists the partial wave components of $s_{1/2}$, $p_{1/2}$, $p_{3/2}$, $d_{5/2}$, $f_{5/2}$, and $g_{9/2}$ at the zero pairing limit ($\Delta = 0$ MeV).

In Figs. 1–3, for those partial wave components, we show the square of the T matrix $|T_{lj}^{(0)}|^2$ in the Fig. 1(a), this is a quantity, which is directly related with the partial wave component of the cross section. The inverse of the K matrix is shown in Fig. 1(b) in order to check the existence of the K -matrix pole on the real axis of the incident energy. In Fig. 1(c), the phase shift, which is determined by the S matrix as $S_{lj}^{(0)} = e^{2i\delta_{lj}^{(0)}}$ is plotted as a function of the incident neutron energy ϵ . The square of the Jost function $|J_{0,lj}^{(+)}(\epsilon)|^2$ are shown on the complex- ϵ plane in order to show the S -matrix pole.

Note that the same Woods-Saxon parameters, which were used in Ref. [7], are adopted in this paper. The chemical potential $\lambda = -8.0$ MeV for the stable nucleus and $\lambda = -1.0$ MeV for the unstable nucleus are adopted unless specifically mentioned.

In Fig. 1, the K -matrix pole is found at $\epsilon_n^0 = 7.81$ MeV for $f_{5/2}$, $\epsilon_n^0 = 9.48$ MeV for $g_{9/2}$, respectively. These energies of poles are corresponding to the peaks of $|T_{lj}^{(0)}|^2$. At $\epsilon = \epsilon_n^0$, the phase shift becomes $\delta_0 = \frac{\pi}{2}$. In Fig. 1(d), we can find the S -matrix pole at $\epsilon_R^0 = 6.75 - i1.63$ MeV for $f_{5/2}$ and $\epsilon_R^0 = 9.06 - i1.14$ MeV for $g_{9/2}$, respectively. However, ϵ_n is slightly different from the real part of the S -matrix pole $\epsilon_R^{0,r}$.

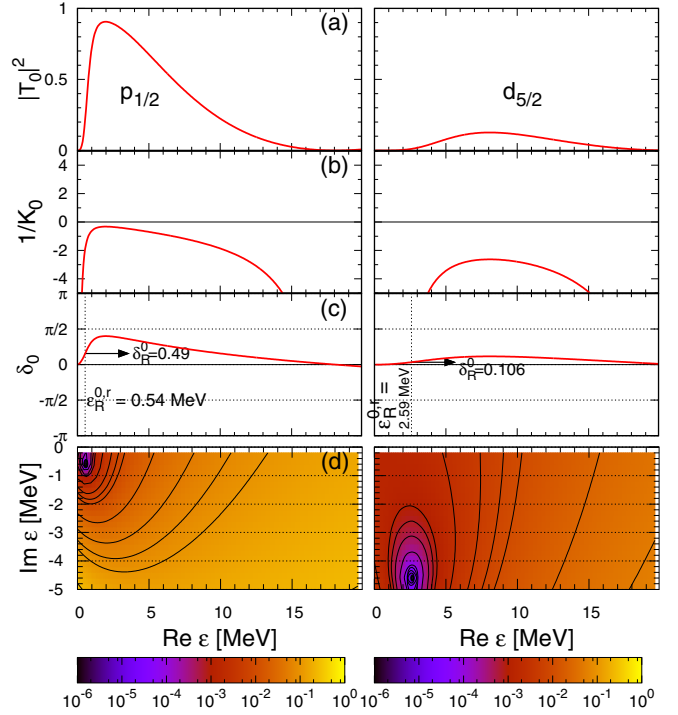


FIG. 2. The same as Fig. 1 but for $p_{1/2}$ and $d_{5/2}$.

In Fig. 2, we can find the S -matrix poles at $\epsilon = 0.54 - i0.56$ and $2.59 - i4.63$ MeV for $p_{1/2}$ and $d_{5/2}$, respectively. However, no K matrix is found in the Fig. 2(b). In the Fig. 2(a), we

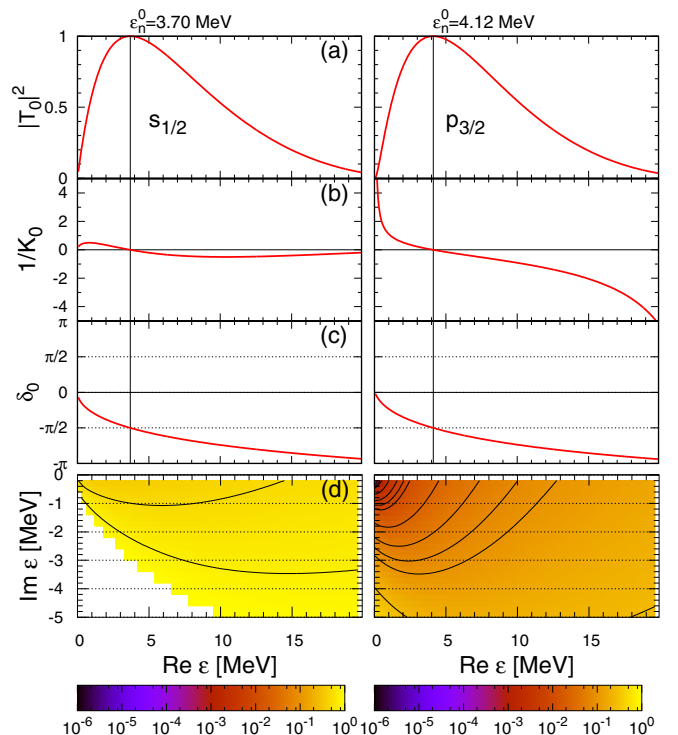


FIG. 3. The same as Fig. 1 but for $s_{1/2}$ and $p_{3/2}$.

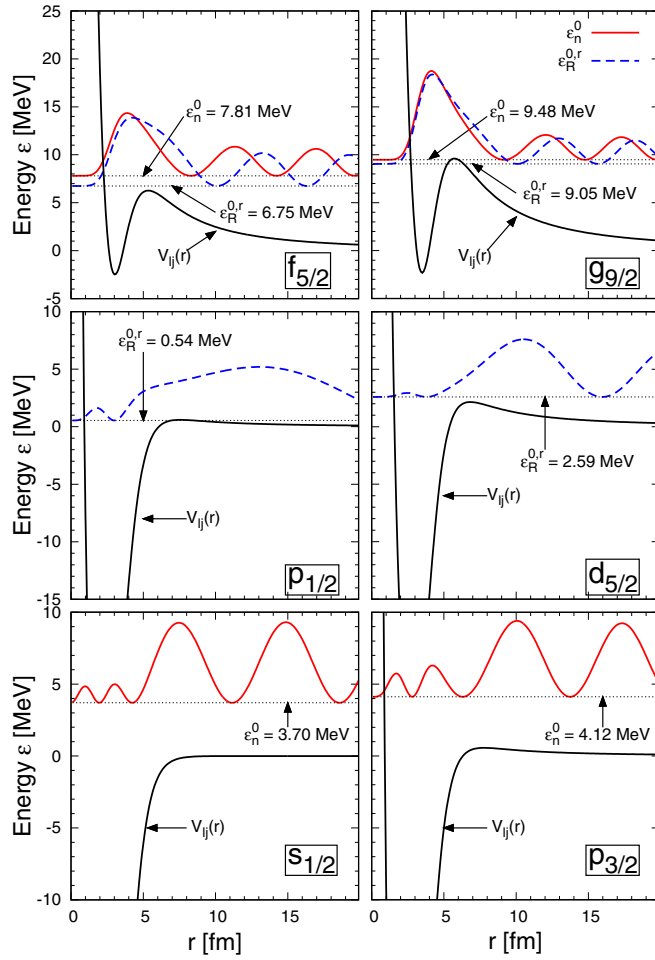


FIG. 4. The square of the scattering wave function $|\psi_{0,lj}^{(+)}|^2$. $V_{ij}(r)$ is the potential defined by $V_{ij}(r) = U_{ij}(r) + \hbar^2 l(l+1)/2mr^2$. The solid red and dashed blue curves are the square of the wave function at $\epsilon = \epsilon_n^0$ and $\epsilon_R^{0,r}$, respectively.

can see the broad peak shape of square of the T matrix, but obviously the peak energy is quite different from $\epsilon_R^{0,r}$.

In Fig. 3, we can find the K -matrix pole at $\epsilon_n^0 = 3.70$ and 4.12 MeV for $s_{1/2}$ and $p_{3/2}$, respectively. These poles are corresponding to the peaks of $|T_{ij}^{(0)}|^2$, but different shape from the typical resonance formula. The phase shift shows the smooth profile as a function of the energy although it goes through $\pi/2$ at $\epsilon = \epsilon_n^0$. No S -matrix pole is found in the Fig. 3(d). This may be a typical profile of the standing wave solution.

The square of the wave functions $|\psi_{0,lj}^{(+)}|^2$ are shown in Fig. 4 together with the potential $V_{ij}(r) = U_{ij}(r) + \hbar^2 l(l+1)/2mr^2$ (the solid black curve). For $f_{5/2}$ and $g_{9/2}$, the amplitude at the internal region of the potential is larger than the one at the outside of the potential. The wave function, which exhibits the internal structure in the nucleus, is connected with the free particle states outside the nucleus asymptotically. This behavior shows the metastable property of the state. Both the S - and K -matrix poles for $f_{5/2}$ and $g_{9/2}$ are found near the top of the centrifugal barrier of the potential. These properties exhibit the typical properties of those so-called written in many

textbooks. The K -matrix poles of $s_{1/2}$ and $p_{3/2}$ are found at the continuum energy region. The behavior of the wave function exhibits a typical behavior of the standing wave solution, and the wave length of the wave function inside of the potential is reflected by the potential depth. The outer amplitude is larger than the inner one. The S -matrix poles for $p_{1/2}$ and $d_{5/2}$ are found near the top of the centrifugal barrier although the height of the barrier is very low. The amplitude of square of the wave function outside the potential is much larger than the one inside the potential, even though the imaginary part of the S -matrix pole for $p_{1/2}$ is small. As one can see in Fig. 2, the phase shift is very small at $\epsilon = \epsilon_R^{0,r}$ for $p_{1/2}$ and $d_{5/2}$. This means that the interference between the scattering wave and outgoing wave without scattering is very small. Namely, the incident wave can not enter the nucleus at $\epsilon = \epsilon_R^{0,r}$ for $p_{1/2}$ and $d_{5/2}$ even though the centrifugal barrier is very small.

Summarizing the analysis of Figs. 1–4, we can conclude about the scattering solution and resonance on n - A scattering within the HF framework as following:

- (i) The S -matrix and K -matrix poles can exist independently.
- (ii) In order to form a resonance, the real part of the pole of the S matrix is necessary to be near the pole of the K matrix. It is found that the scattering wave function has the metastable structure. Hereafter, we call this type scattering solution as the resonance.
- (iii) The independent S -matrix pole can not form the resonance by itself. The square of the T matrix has the broad shape and less contribution than others. The wave function has the larger amplitude outside of nucleus than inside. It seems that the incident wave can not enter the nucleus even if the centrifugal barrier is small.
- (iv) The independent K -matrix pole exhibits the standing wave solution. The square of the T matrix at the energy of the K -matrix pole has a peak, but the shape is different from the Breit-Wigner formula.

In the next section, we will analyze the pairing dependence of the scattering solutions (resonance, independent S - and K -matrix poles) within the HFB framework.

B. S and K matrix and scattering states of n - A scattering with pairing

In order to show the pairing dependence of poles of the S and K matrix, it is necessary to introduce the definition of the S and K matrix, which are described within the HFB framework. Within the HFB formalism, the S , T , and K matrix are represented by using the HFB Jost function as

$$S_{ij}(E) = \frac{\det \mathcal{J}_{ij}^{(+)*}(E^*)}{\det \mathcal{J}_{ij}^{(+)}(E)} \quad (7)$$

$$T_{ij}(E) = \frac{i}{2}(S_{ij}(E) - 1) \quad (8)$$

$$= \frac{i}{2} \left(\frac{\det \mathcal{J}_{ij}^{(+)*}(E^*) - \det \mathcal{J}_{ij}^{(+)}(E)}{\det \mathcal{J}_{ij}^{(+)}(E)} \right), \quad (9)$$

and the K matrix is

$$K_{lj}(E) = \frac{T_{lj}(E)}{1 - iT_{lj}(E)} \quad (10)$$

$$= i \left(\frac{\det \mathcal{J}_{lj}^{(+)*}(E^*) - \det \mathcal{J}_{lj}^{(+)}(E)}{\det \mathcal{J}_{lj}^{(+)*}(E^*) + \det \mathcal{J}_{lj}^{(+)}(E)} \right). \quad (11)$$

The incident energy ϵ and the quasiparticle energy E are related as

$$\epsilon = \lambda + E, \quad (12)$$

where $\lambda (< 0)$ is the chemical potential (Fermi energy) given in the HFB framework. The S -matrix and K -matrix poles are found at $E = E_R$, and E_n , which are determined by

$$\det \mathcal{J}_{lj}^{(+)}(E_R) = 0 \quad (13)$$

and

$$\det \mathcal{J}_{lj}^{(+)*}(E_n) + \det \mathcal{J}_{lj}^{(+)}(E_n) = 0, \quad (14)$$

respectively. It should be noted that the S -matrix pole for a bound state is found on the real axis of the first Riemann sheet of the complex energy E plane, the S -matrix pole for a resonance is found on the second Riemann sheet as a complex energy $E_R (= E_R^r - iE_R^i)$. The K -matrix pole E_n is found on the branch cut, which connects the first and second Riemann sheet (the real axis of E for $E > -\lambda$), since the K matrix is Hermitian.

In order to analyze the pairing effect, the two potential formula is useful. As is introduced in Ref. [17], the S matrix and T matrix can be divided into the HF and pairing parts as

$$S_{lj}(E) = S_{lj}^{(0)}(E)S_{lj}^{(1)}(E) \quad (15)$$

$$T_{lj}(E) = T_{lj}^{(0)}(E) + T_{lj}^{(1)}(E)S_{lj}^{(0)}(E), \quad (16)$$

when the HFB potential $\mathcal{U}_{lj} = \begin{pmatrix} U_{lj} & \Delta \\ \Delta & -U_{lj} \end{pmatrix}$ is divided the HF potential part and pairing part as $\mathcal{U}_{lj} = \mathcal{U}_{lj}^{(0)} + \mathcal{U}_{lj}^{(1)}$ where $\mathcal{U}_{lj}^{(0)} = \begin{pmatrix} U_{lj} & 0 \\ 0 & -U_{lj} \end{pmatrix}$ and $\mathcal{U}_{lj}^{(1)} = \begin{pmatrix} 0 & \Delta \\ \Delta & 0 \end{pmatrix}$.

By inserting Eq. (16) into Eq. (10), we obtain

$$K_{lj}(E) = \frac{K_{lj}^{(0)}(E) + K_{lj}^{(1)}(E)}{1 - K_{lj}^{(0)}(E)K_{lj}^{(1)}(E)} \quad (17)$$

with

$$K_{lj}^{(0)}(E) = \frac{T_{lj}^{(0)}(E)}{1 - iT_{lj}^{(0)}(E)} \quad (18)$$

$$K_{lj}^{(1)}(E) = \frac{T_{lj}^{(1)}(E)}{1 - iT_{lj}^{(1)}(E)}. \quad (19)$$

By using Eqs. (15) and (17), we will classify the scattering solutions as following:

- (i) *Shape resonance*. If the real part of the S -matrix pole originates from the $S_{lj}^{(0)}$ pole is found near the K -matrix pole originates from the $K_{lj}^{(0)}$ pole, it is called the shape resonance.

- (ii) *Quasiparticle (qp) resonance*. If the real part of the S -matrix pole originates from the $S_{lj}^{(1)}$ pole is found near the K -matrix pole originates from the $K_{lj}^{(1)}$ pole, it is called the quasiparticle resonance. If the quasiparticle resonance originates from the bound particle (or hole) state, it is called the particle-type (or hole-type) quasiparticle resonance.

- (iii) *Independent S -matrix pole*. If no K -matrix pole is found near the real part of the S -matrix pole E_R , the S -matrix pole is called the independent S -matrix pole.

- (iv) *Independent K -matrix pole* (standing wave solution). If the K -matrix pole is not close to the real part of the pole of the S matrix and also it originates from the pole of $K_{lj}^{(0)}$, it is called the pole of the independent K matrix. This has a physical meaning as a standing wave.

In Figs. 5–7, the S -matrix poles E_R and K -matrix poles E_n are plotted as a function of the mean pairing gap $\langle \Delta \rangle$ within the range $0 \leq \langle \Delta \rangle \leq 10$ MeV. The S -matrix pole E_R for the bound state can be found on the real axis of the first Riemann sheet by solving Eq. (13) numerically. The E_R of the resonance (or independent S -matrix poles) can be found as a complex energy solution in the second Riemann sheet. The E_R for the bound state, which is given by the real number, is represented by the black cross symbols. The E_R found on the second Riemann sheet given by the complex number is represented by the unfilled red circles or triangles with the error bars, the unfilled symbols and error bars represent the real (E_R^r) and imaginary part (E_R^i), respectively. The K -matrix poles E_n are found on the branch cut (the real axis for $E > -\lambda$) as the numerical solution of Eq. (13). Those are shown by the filled blue circles or triangles. As shown in Eqs. (15) and (17), the S and K matrices are represented by mean-field component ($S_{lj}^{(0)}$, $K_{lj}^{(0)}$) and pairing component ($S_{lj}^{(1)}$, $K_{lj}^{(1)}$), respectively. To distinguish the contribution of these components in figures, the poles originating from the mean-field component are represented by circles and those originating from the pairing component are represented by triangles. The results for the stable target of nucleus ($\lambda = -8.0$ MeV) are shown in Fig. 5. Figures 6 and 7 are results for the unstable target of nucleus ($\lambda = -1.0$ MeV).

1. Analysis of $f_{5/2}$ and $g_{9/2}$

In the top panels of Figs. 5 and 6, we can find the shape resonances for $f_{5/2}$ and $g_{9/2}$ and their pairing dependence. We can see the small difference between the pairing dependence of the S - and K -matrix poles. The pairing effect is very small for the S -matrix pole, especially the real part of pole is almost constant for varying the pairing gap. On the other hand, the K -matrix pole is shifted to higher energy as the pairing gap increases.

Since the S matrix is expressed by Eq. (15), the S -matrix pole is given by the pole of $S_{lj}^{(0)}$, i.e.,

$$E_R \approx E_R^{(0)}. \quad (20)$$

However, one can find that the pairing has some small effect to make the imaginary part of the S -matrix pole larger when

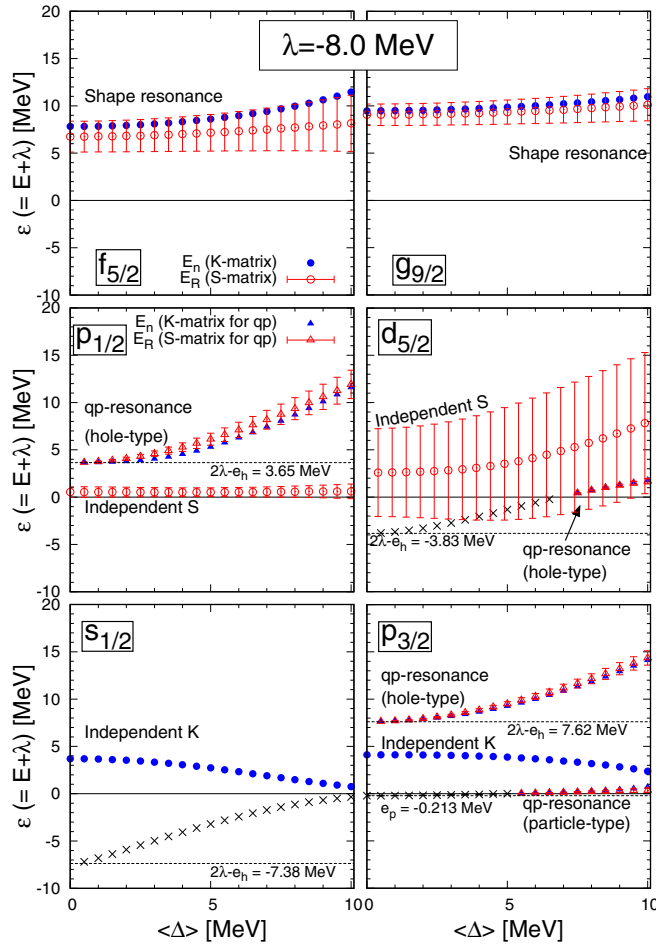


FIG. 5. The S - and K -matrix poles (E_R and E_n) plotted as a function of the mean pairing gap $\langle\Delta\rangle$ with $\lambda = -8.0$ MeV (stable nucleus). The S -matrix poles for the bound state is represented by the black cross symbols. The S -matrix poles are found in the scattering energy region ($\epsilon = E + \lambda > 0$) as the complex energy $E_R = E_R^r - iE_R^i$, E_R^r is represented by the unfilled red symbols (circles and triangles), and E_R^i is represented by the red error bars. The filled blue symbols (circles and triangles) represent the K -matrix poles E_n . The circle and triangle symbols represent the poles originate from the mean field components ($S_{ij}^{(0)}$ or $K_{ij}^{(0)}$) and the pairing components ($S_{ij}^{(1)}$ or $K_{ij}^{(1)}$), respectively. See text for details.

the pairing is very strong. This effect is expected from the higher-order contribution of the pairing effect.

Since the K matrix is expressed by Eq. (17), it is clear that the K -matrix pole E_n is determined as, i.e.,

$$K_{ij}^{(1)}(E_n) = 1/K_{ij}^{(0)}(E_n). \quad (21)$$

By using the first-order approximation of the Taylor expansion, the inverse of $K_{ij}^{(0)}(E)$ can be expressed as

$$\frac{1}{K_{ij}^{(0)}(E)} \approx \frac{E - E_n^{(0)}}{c_{ij}^{(0)}}, \quad (22)$$

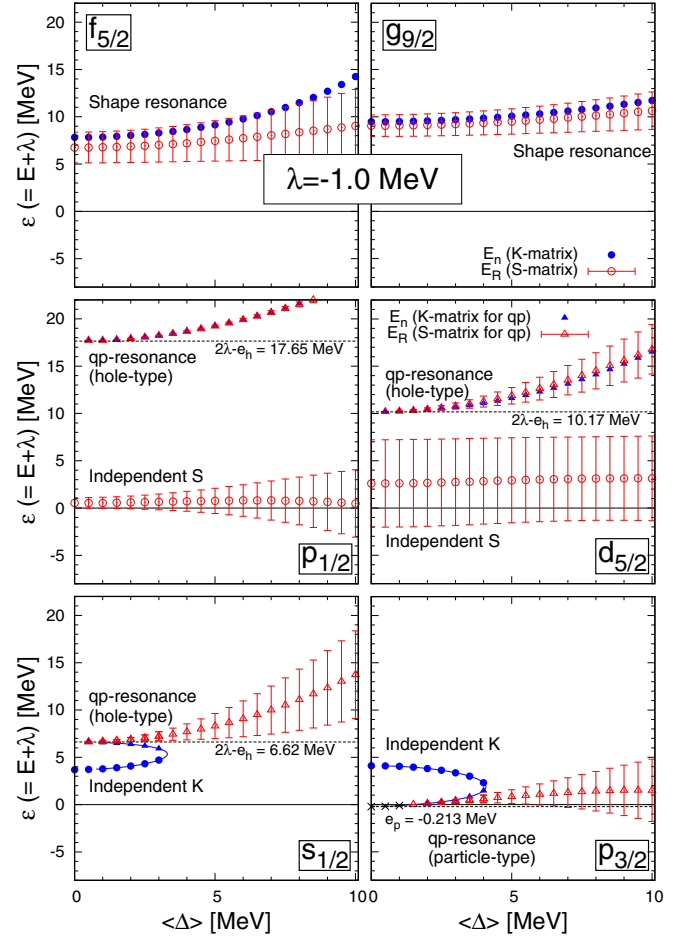


FIG. 6. The same as Fig. 5 but $\lambda = -1.0$ MeV (unstable nucleus).

where c_{ij} is a real number defined by

$$\frac{1}{c_{ij}^{(0)}} = \left(\frac{d}{dE} \frac{1}{K_{ij}^{(0)}(E)} \right)_{E=E_n^{(0)}}. \quad (23)$$

By inserting Eq. (22) into Eq. (21), we can obtain

$$E_n \approx E_n^{(0)} + c_{ij}^{(0)} K_{ij}^{(1)}(E_n). \quad (24)$$

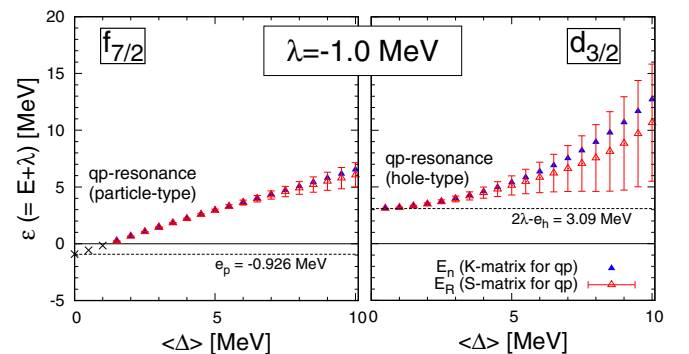


FIG. 7. The same as Fig. 5 but for $f_{7/2}$ and $d_{3/2}$ with $\lambda = -1.0$ MeV (unstable nucleus).

This is the qualitative explanation about the difference of the pairing dependence for the shape resonance seen in the top panels of Figs. 5 and 6.

2. Analysis of $p_{1/2}$ and $d_{5/2}$

In the middle panels of Figs. 5 and 6, a hole-type qp resonance and an independent S -matrix pole are found for $p_{1/2}$ and $d_{5/2}$. The small pairing approximation of $S_{ij}^{(1)}$ and $K_{ij}^{(1)}$ are derived in Appendix B and are given by Eqs. (B7) and (B13), respectively. Since the S matrix S_{ij} is described by Eq. (15), the $S_{ij}^{(0)}$ and $S_{ij}^{(1)}$ are not correlated to each other as long as Eqs. (B7) and (B13) are in good approximation. Therefore, the S -matrix pole E_R is given by

$$E_R \approx E_R^{(1)}, \quad (25)$$

where $E_R^{(1)}$ is given by Eq. (B14). By inserting Eq. (B13) into Eq. (21), we can obtain the K -matrix pole E_n as

$$E_n \approx E_n^{(1)} + K_{ij}^{(0)}(E)\Gamma_{ij}^{(h)}(E), \quad (26)$$

where $E_n^{(1)}$ and $\Gamma_{ij}^{(h)}(E)$ are given by Eqs. (B15) and (B10). The difference between $\text{Re } E_R$ and E_n is due to the second term of Eq. (26). This is the qualitative explanation of the difference $\text{Re } E_R$ and E_n for the qp resonance shown in the middle panels of Figs. 5 and 6.

The pairing effect on the independent S matrix, which is seen for $d_{5/2}$ with $\lambda = -8.0$ MeV and $p_{1/2}$ with $\lambda = -1.0$ MeV, is due to the higher-order correction of the pairing. In the case of $d_{5/2}$ with $\lambda = -8.0$ MeV, it seems that a hole-type quasiparticle state pushes up the independent S -matrix pole. This is the origin of the different behavior of the $d_{5/2}$ trajectory from others as shown in Fig. 9 of Ref. [7].

3. Analysis of $s_{1/2}$ and $p_{3/2}$

In the bottom panels of Figs. 5 and 6, we can find the independent K -matrix pole and the qp resonance for $s_{1/2}$ and $p_{3/2}$. From Eq. (21), it is clear that both $K_{ij}^{(0)}$ and $K_{ij}^{(1)}$ are strongly correlated to each other when both of them have the poles.

By inserting Eq. (22) into Eq. (21) and using Eq. (B13) (for hole-type) or (B24) (for particle-type), we can obtain

$$(E_n - E_n^{(0)})(E_n - E_n^{(1)}) = c_{ij}^{(0)}\Gamma_{ij}^{(h \text{ or } p)}/2, \quad (27)$$

where $E_n^{(1)}$ is the pole of $K_{ij}^{(1)}$ [given by Eqs. (B13) or (B24)]. In order for Eq. (27) to be obtained for a particle-type resonance, $\frac{E-E_p^0}{E+E_p^0} \approx 1$ [this factor appears in Eqs. (B18) and (B24)] must be satisfied. This condition required for the system is exactly that of a neutron-rich unstable nucleus, and is reasonable condition to explain the case of $p_{3/2}$ shown in the bottom right panel of Fig. 6. By supposing that the energy dependence of F_{ij} and Γ_{ij} (defined in Appendix B) is small, it is clear that one can find two solutions of Eq. (27). Both $E_n^{(1)}$ and Γ_{ij} increase as the pairing gap increases. Therefore, critical pairing gap $\langle \Delta \rangle_c$ can be defined as the pairing gap when the discriminant of Eq. (27) is zero, i.e.,

$$(E_n^{(0)} + E_n^{(1)})^2 - 4(E_n^{(0)}E_n^{(1)} - c_{ij}^{(0)}\Gamma_{ij}/2) = 0. \quad (28)$$

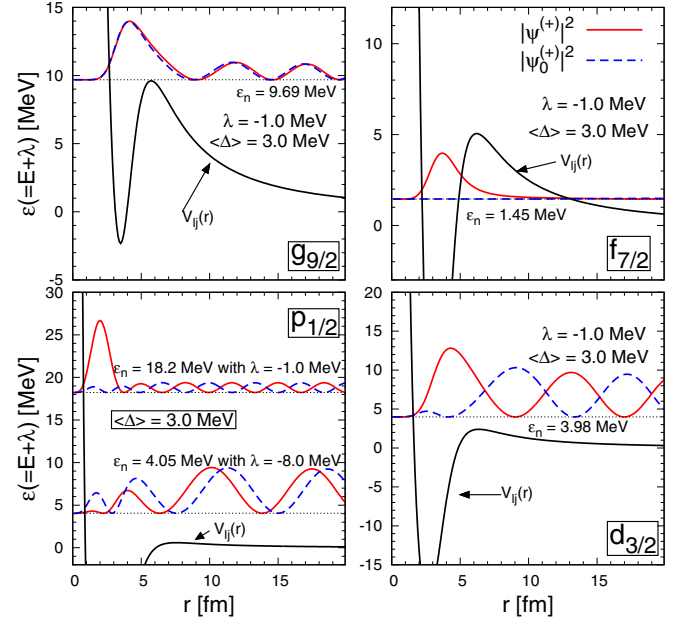


FIG. 8. The square of the scattering wave functions for resonances. The upper component of the HFB scattering wave function $|\psi_1^{(+)}|^2$, and HF scattering wave function $|\psi_0^{(+)}|^2$ are plotted as a function of r [fm] by the red solid and blue dashed curves, respectively. The HF potential $V_{ij} = U_{ij} + \hbar^2 l(l+1)/2mr^2$ is plotted together by the black solid curve. See text for details.

When $\langle \Delta \rangle = \langle \Delta \rangle_c$, E_n is given by $E_n = \frac{1}{2}(E_n^{(0)} + E_n^{(1)})$, and E_n doesn't exist for $\langle \Delta \rangle > \langle \Delta \rangle_c$ because the discriminant becomes negative. The existence of the critical pairing gap $\langle \Delta \rangle_c$ exhibits the breaking effect of the quasiparticle resonance by the independent K -matrix pole and pairing. In the bottom panels of Fig. 6, the critical pairing gap is given by $\langle \Delta \rangle_c = 3.30$ MeV for $s_{1/2}$ (left panel) and $\langle \Delta \rangle_c = 4.08$ MeV for $p_{3/2}$ (right panel), respectively.

4. Analysis of $f_{7/2}$ and $d_{3/2}$

In Fig. 7, we show the quasiparticle resonance for the partial wave components ($f_{7/2}$ and $d_{3/2}$), which do not have any visible contribution of $|T|^2$ at the zero pairing limit (i.e., $|T|^2 \rightarrow |T_0|^2 \approx 0$ with $\langle \Delta \rangle \rightarrow 0$). Figure 7 is a good example to discuss the difference of the pairing effect between the hole-type and particle-type resonance, because there is no correlation by the independent S - or K -matrix pole since $K_{ij}^{(0)} \approx 0$ when $T_{ij}^{(0)} \approx 0$. The S - and K -matrix poles for $f_{7/2}$ and $d_{3/2}$ are expressed directly by $E_R^{(1)}$ and $E_n^{(1)}$ in Appendix B. As is shown by Eqs. (B25) and (B26), the coupling effect with continuum is negligible for the particle-type resonance. This is consistent with our numerical results shown in the left panel of Fig. 7.

5. Analysis of resonance wave function

In Fig. 8, the scattering wave functions of the resonances are plotted as a function of r . The red solid curves represent the square of the upper component of the HFB scattering wave function $|\psi_{1,lj}^{(+)}|^2$, the blue dashed curves are the HF wave

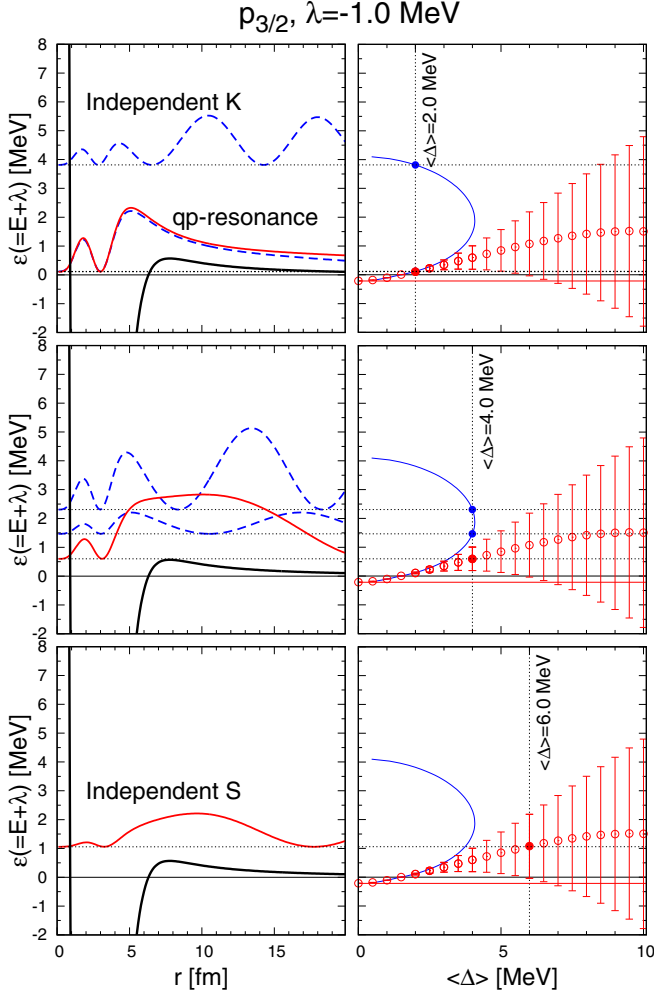


FIG. 9. Pairing gap evolution of the correlation between the qp resonance and the independent K -matrix pole of $p_{3/2}$ with $\lambda = -1.0$ MeV. The S - and K -matrix poles are plotted as a function of the pairing gap $\langle \Delta \rangle$ in the right panels. The real and imaginary part of the S -matrix pole (E_R^r and E_R^i) are represented by the red circles and error-bars, respectively. The K -matrix poles E_n are shown by the blue circles and solid curves. In the left panels, the corresponding wave functions are plotted as a function of r . The wave function at the real part of the S -matrix pole $E = E_R^r$ is represented by the red solid curve, the wave function for the K -matrix pole E_n is represented by the blue dashed curve. The top, middle, and bottom panels are representing figures for $\langle \Delta \rangle = 2.0, 4.0$ and 6.0 MeV, respectively.

function $|\psi_{0,lj}^{(+)}|^2$. The difference of those exhibits the effect of the pairing on the scattering wave function. We can see that the most of the resonance wave functions have the metastable structure except the wave function of the $p_{1/2}$ hole-type qp resonance with $\lambda = -8.0$ MeV. We can not see the clear pairing effect for the shape resonance of $g_{9/2}$. The wave function of the particle-type qp resonance of $f_{7/2}$ with $\lambda = -1.0$ MeV represents almost the characteristics of the bound state. The corresponding peak of the cross section is expected to be a very sharp peak as a bound state embedded in the continuum.

In the bottom left panel of Fig. 8, the wave function of $p_{1/2}$ hole-type qp resonance with $\lambda = -1.0$ and -8.0 MeV

are shown together. The wave function with $\lambda = -1.0$ MeV exhibits the typical behavior of the metastable state, however, the wave function with $\lambda = -8.0$ MeV does not have the metastable structure although the large value of the phase shift is expected from the outer behavior of the wave function. This difference is due to the Fano effect caused by the pairing, which is introduced in Ref. [17]. The Fano effect is the quantum interference effect between the bound state and background continuum. As is known, the shape of the cross section becomes the asymmetric shape and the Breit-Wigner type of shape with the small and large values of q , respectively. The physical meaning of q is the transition probability to the modified quasihole state at the resonance energy. The hole-type qp resonance for $p_{1/2}$ with $\lambda = -8.0$ MeV appears at the energy where the value of q is small. In contrast, the one with $\lambda = -1.0$ MeV appears at the energy where the value of q is large. The wave function of the hole-type qp resonance for $d_{3/2}$ with $\lambda = -1.0$ MeV also has been analyzed in Ref. [17] as an example of the resonance, which has large value of q , and has the metastable structure of the wave function as is shown in the lower right panel of Fig. 8. Therefore, it is found that the large transition probability to the modified quasihole state is necessary to form the metastable structure of the scattering wave function for the hole-type qp resonance. In Fig. 9, we demonstrate how the qp resonance wave function is broken by the wave solution of the independent K -matrix pole. When $\langle \Delta \rangle = 2.0$ MeV, the resonance wave function still keeps the metastable structure. As the pairing increases, the resonance wave function is separated into the wave functions for the S -matrix pole and the K -matrix pole. The K -matrix pole originates when the qp resonance and the independent one approach each other and vanishes when $\langle \Delta \rangle = \langle \Delta \rangle_c$. The metastable structure of the qp resonance wave function is broken and is changed to the wave function structure of the independent S -matrix pole.

III. SUMMARY

We have investigated the pairing effect of n - A -scattering solutions within the HFB framework. In order to analyze the pairing effect, we classified the scattering solutions in terms of the S - and K -matrix poles. By applying the two potential formula, we divided the S and K matrix into two parts, the HF part ($S_{ij}^{(0)}, K_{ij}^{(0)}$) and pairing part ($S_{ij}^{(1)}, K_{ij}^{(1)}$). The shape resonance is defined when the poles of the $S_{ij}^{(0)}$ and $K_{ij}^{(0)}$ are in close proximity to each other. The quasiparticle (qp) resonance is defined by the poles of the $S_{ij}^{(1)}$ and $K_{ij}^{(1)}$, which are in close proximity to each other. Since it originates from the bound particle (or hole) state, it is called as the particle (or hole)-type qp resonance. The independent K -matrix pole, which has the physical meaning as the standing wave solution originates from the pole of $K_{ij}^{(0)}$. Analyzing all of those scattering solutions, we found the following:

- (i) The pairing effect on the shape resonance is negligibly small.
- (ii) The pairing dependence of the particle-type and hole-type qp resonance is slightly different. The hole-type

qp resonance is more sensitive to the coupling effect with continuum than the particle-type resonance.

- (iii) Basically, all kinds of the resonance have the metastable structure of the wave function except the following cases.
- (iv) The independent K -matrix pole correlates with the qp resonance. The correlation destroys the metastable structure of the qp resonance, and transforms the qp resonance into the independent S -matrix pole.
- (v) The presence of independent S -matrix poles in the vicinity of a hall-type qp resonance will destroy the metastable structure of the qp resonance, while maintaining the phase shift property for asymmetric

behavior of the wave function. This can be considered to be another aspect of the Fano effect.

Finally, it can be concluded that, although the shape resonance, particle-type qp resonance and independent S -matrix poles were classified as the same particle-type S -matrix pole in Ref. [7], they have different properties and should be classified as different scattering states.

ACKNOWLEDGMENT

This work is funded by Vietnam National Foundation for Science and Technology Development (NAFOSTED) under Grant No. "103.04-2019.329".

APPENDIX A: EQUIVALENCY OF THE K -MATRIX POLES AND EIGENSOLUTIONS OF THE STRUM-LIOUVILLE THEORY

Within the HF framework, the Lippmann-Schwinger equation is given by

$$\psi_{0,l_j}^{(+)}(r; \epsilon) = F_l(kr) + \int_0^\infty dr' G_{F,l}^{(+)}(r, r'; k) U_{l_j}(r') \psi_{0,l_j}^{(+)}(r'; \epsilon) \quad (\text{A1})$$

with the HF potential U_{l_j} , where ϵ is the incident energy ($\epsilon = \frac{\hbar^2 k^2}{2m}$) and $G_{F,l}^{(\pm)}(r, r'; \epsilon)$ is the free particle Green's function defined by

$$G_{F,l}^{(\pm)}(r, r'; k) \equiv \mp i \frac{2mk}{\hbar^2} [\theta(r-r') F_l(kr') O_l^{(\pm)}(kr) + \theta(r'-r) F_l(kr) O_l^{(\pm)}(kr')]. \quad (\text{A2})$$

With the scaled riccati-spherical Bessel functions defined by $F_l(kr) = r j_l(kr)$ and $O_l^{(\pm)}(kr) = r h_l^{(\pm)}(kr) = r j_l(kr) \pm i r n_l(kr)$, where $n_l(kr)$ is the spherical Neumann function.

By introducing the standing wave Green's function $PG_{F,l}$ defined by

$$G_{F,l}^{(\pm)}(r, r'; k) = PG_{F,l}(r, r'; k) \mp i \frac{2mk}{\hbar^2} F_l(kr) F_l(kr'), \quad (\text{A3})$$

Eq. (A1) can be rewritten as

$$\psi_{0,l_j}^{(+)}(r; \epsilon) = (1 - iT_{l_j}^{(0)}(\epsilon)) F_l(kr) + \int_0^\infty dr' PG_{F,l}(r, r'; k) U_{l_j}(r') \psi_{0,l_j}^{(+)}(r'; \epsilon), \quad (\text{A4})$$

where $T_{l_j}^{(0)}$ is the T matrix within the HF framework, which can be calculated by

$$T_{l_j}^{(0)}(\epsilon) = \frac{2mk}{\hbar^2} \int_0^\infty dr F_l(kr) U_{l_j}(r) \psi_{0,l_j}^{(+)}(r; \epsilon). \quad (\text{A5})$$

The K matrix $K_{l_j}^{(0)}$ is expressed by the T matrix $T_{l_j}^{(0)}$ as

$$K_{l_j}^{(0)}(\epsilon) = \frac{T_{l_j}^{(0)}(\epsilon)}{1 - iT_{l_j}^{(0)}(\epsilon)}, \quad (\text{A6})$$

and the standing wave function $\psi_{0,l_j}^{(S)}(r; \epsilon)$ is defined by

$$\psi_{0,l_j}^{(S)}(r; \epsilon) \equiv (1 + iK_{l_j}^{(0)}(\epsilon)) \psi_{0,l_j}^{(+)}(r; \epsilon) \quad (\text{A7})$$

$$\equiv \frac{1}{1 - iT_{l_j}^{(0)}(\epsilon)} \psi_{0,l_j}^{(+)}(r; \epsilon). \quad (\text{A8})$$

Equation (A4) can be rewritten as

$$\psi_{0,l_j}^{(S)}(r; \epsilon) = F_l(kr) + \int_0^\infty dr' PG_{F,l}(r, r'; k) U_{l_j}(r') \psi_{0,l_j}^{(S)}(r'; \epsilon). \quad (\text{A9})$$

If there is an energy ϵ_n^0 , which is given by

$$1 - iT_{l_j}^{(0)}(\epsilon_n^0) = 0 \quad (\text{A10})$$

or

$$1/K_{lj}^{(0)}(\epsilon_n^0) = 0, \quad (\text{A11})$$

then Eq. (A9) can be rewritten as

$$\psi_{0,lj}^{(+)}(r; \epsilon_n^0) = \int_0^\infty dr' P G_{F,l}(r, r'; k_n^0) U_{lj}(r') \psi_{0,lj}^{(+)}(r'; \epsilon_n^0). \quad (\text{A12})$$

using Eq. (A8), also ϵ_n^0 is a pole of the K matrix by Eq. (A6).

The Sturm-Liouville theory [23] is the theory of the second-order differential equations of the form:

$$\frac{\partial}{\partial r} \left[p(r) \frac{\partial \hat{\phi}(r)}{\partial r} \right] + q(r) \hat{\phi}(r) = -\nu w(r) \hat{\phi}(r), \quad (\text{A13})$$

where $p(r)$, $q(r)$, and $w(r)$ are positive definite coefficient functions. For the HF equation, the coefficient functions are given by

$$p(r) = \frac{\hbar^2}{2m} \quad (\text{A14})$$

$$q(r) = \epsilon - \frac{\hbar^2 l(l+1)}{2mr^2} \quad (\text{A15})$$

$$w(r) = -U_{lj}(r), \quad (\text{A16})$$

when $\epsilon > 0$. ν is called the eigenvalue of the Sturm-Liouville equation. According to the Sturm-Liouville theory, there are an infinite number of real eigenvalues ν_n , which can be numbered so that $\nu_1 < \nu_2 < \dots < \nu_\infty$ (Mercer's theorem [24]). An eigenfunction $\hat{\phi}_{n,lj}(r)$ has $n-1$ nodes inside the potential. Note that the orthogonality of $\hat{\phi}_{n,lj}$ is given by

$$\int_0^\infty dr \hat{\phi}_{m,lj}(r) w(r) \hat{\phi}_{n,lj}(r) = \delta_{mn}. \quad (\text{A17})$$

Completeness is given by

$$\sum_{n=1}^\infty w(r) \hat{\phi}_{n,lj}(r) \hat{\phi}_{n,lj}(r') = \sum_{n=1}^\infty \hat{\phi}_{n,lj}(r) \hat{\phi}_{n,lj}(r') w(r') = \delta(r - r'). \quad (\text{A18})$$

The eigensolution $\hat{\phi}_{n,lj}$ satisfies

$$\hat{\phi}_{n,lj}(r) = \int_0^\infty dr' P G_{F,l}(r, r'; k) \nu_n U_{lj}(r') \hat{\phi}_{n,lj}(r'). \quad (\text{A19})$$

If we suppose that there is an eigenvalue, which satisfies $\nu_n(\epsilon = \epsilon_n^0) = 1$, it is very easy to notice that Eqs. (A12) and (A19) are equivalent. Therefore, the K -matrix pole is same with the eigenvalue of the Sturm-Liouville eigenvalue problem.

APPENDIX B: TWO POTENTIAL FORMULA FOR THE HFB JOST FUNCTION AND S AND K MATRICES

By using the two potential formula for the HFB Jost function, the determinant of the HFB Jost function can be expressed as

$$\begin{aligned} \det(\mathcal{J}_{lj}^{(+)}(E)) &= (\mathcal{J}_{lj}^{(+)}(E))_{22} \left[J_{0,lj}^{(+)}(k_1(E)) \right. \\ &\quad \left. + \frac{2m}{\hbar^2} \frac{k_1(E)}{i} \int \int_0^\infty dr dr' \varphi_{0,lj}^{(+)}(r; k_1(E)) \Delta(r) G_{HF,lj}(r, r'; k_2(E)) \Delta(r') \phi_{1,lj}(r'; E) \right], \end{aligned} \quad (\text{B1})$$

where $J_{0,lj}^{(+)}$, $\varphi_{0,lj}^{(+)}$, and $G_{HF,lj}$ is the HF Jost function, irregular solution and Green's function. $\Delta(r)$ is the pairing potential. $k_1(E)$ and $k_2(E)$ are defined by

$$k_1(E) = \sqrt{\frac{2m}{\hbar^2}(\lambda + E)} \quad (\text{B2})$$

$$k_2(E) = \sqrt{\frac{2m}{\hbar^2}(\lambda - E)}, \quad (\text{B3})$$

respectively. $\phi_{1,lj}$ is the upper component of the regular solution of the HFB equation, which is defined by the linear combination of two kinds of the regular solution $\phi_{lj}^{(r1)}(r; E)$ and $\phi_{lj}^{(r2)}(r; E)$ as

$$\phi_{lj}(r; E) = \begin{pmatrix} \phi_{1,lj}(r; E) \\ \phi_{2,lj}(r; E) \end{pmatrix} = \phi_{lj}^{(r1)}(r; E) - \frac{(\mathcal{J}_{lj}^{(+)}(E))_{12}}{(\mathcal{J}_{lj}^{(+)}(E))_{22}} \phi_{lj}^{(r2)}(r; E). \quad (\text{B4})$$

By applying Eqs. (B1) to (7), we can obtain

$$S_{lj}^{(1)}(E) = \frac{1 + i \frac{2m}{\hbar^2} \frac{k_1(E)}{J_{0,lj}^{(-)}(k_1(E))} \langle \varphi_{0,lj}^{(-)} | \Delta G_{HF,lj}(k_2(E)) \Delta | \phi_{1,lj} \rangle}{1 - i \frac{2m}{\hbar^2} \frac{k_1(E)}{J_{0,lj}^{(+)}(k_1(E))} \langle \varphi_{0,lj}^{(+)} | \Delta G_{HF,lj}(k_2(E)) \Delta | \phi_{1,lj} \rangle}, \quad (\text{B5})$$

where

$$\langle \varphi_{0,lj}^{(\pm)} | \Delta G_{HF,lj}(k_2(E)) \Delta | \phi_{1,lj} \rangle \equiv \int \int_0^\infty dr dr' \varphi_{0,lj}^{(\pm)}(r; k_1(E)) \Delta(r) G_{HF,lj}(r, r'; k_2(E)) \Delta(r') \phi_{1,lj}(r'; E). \quad (\text{B6})$$

Note that we do not use any approximation to derive Eq. (B5) within the HFB framework.

1. Hole-type quasiparticle resonance

By supposing only one bound hole state in the system, Eq. (B5) is expressed as

$$S_{lj}^{(1)}(E) \approx \frac{E - E_h^0 - \frac{\langle \phi_{h,lj} | \Delta | \phi_{h,lj} \rangle^2}{E + E_h^0} - W_{lj}^{(h)*}(E)}{E - E_h^0 - \frac{\langle \phi_{h,lj} | \Delta | \phi_{h,lj} \rangle^2}{E + E_h^0} - W_{lj}^{(h)}(E)}, \quad (\text{B7})$$

where

$$W_{lj}^{(h)}(E) = F_{lj}^{(h)}(E) - i\Gamma_{lj}^{(h)}(E)/2 \quad (\text{B8})$$

$$F_{lj}^{(h)}(E) = \frac{2m}{\hbar^2} \frac{2}{\pi} P \int_0^\infty dk' k'^2 \frac{|\langle \psi_{0,lj}^{(+)}(k') | \Delta | \phi_{h,lj} \rangle|^2}{k_1^2(E) - k'^2}, \quad (\text{B9})$$

$$\Gamma_{lj}^{(h)}(E)/2 = \frac{2mk_1(E)}{\hbar^2} |\langle \psi_{0,lj}^{(+)}(k_1(E)) | \Delta | \phi_{h,lj} \rangle|^2, \quad (\text{B10})$$

$$E_h^0 = \lambda - e_h (> 0) \quad (\text{B11})$$

as the weak pairing approximation.

By using Eq. (B7), $T_{lj}^{(1)}$ and $K_{lj}^{(1)}$ can be obtained as

$$T_{lj}^{(1)}(E) = \frac{\Gamma_{lj}^{(h)}(E)/2}{E - E_h^0 - \frac{\langle \phi_{h,lj} | \Delta | \phi_{h,lj} \rangle^2}{E + E_h^0} - W_{lj}^{(h)}(E)}, \quad (\text{B12})$$

$$K_{lj}^{(1)}(E) = \frac{\Gamma_{lj}^{(h)}(E)/2}{E - E_h^0 - \frac{\langle \phi_{h,lj} | \Delta | \phi_{h,lj} \rangle^2}{E + E_h^0} - F_{lj}^{(h)}(E)}. \quad (\text{B13})$$

Note that $F_{lj}^{(h)}$ and $\Gamma_{lj}^{(h)}$ are expected to be zero when $\epsilon = E + \lambda < 0$. Therefore, the pole of $S_{lj}^{(1)}$, $E_R^{(1)}$ is given by

$$E_R^{(1)} \approx \begin{cases} \sqrt{(E_h^0)^2 + \langle \phi_{h,lj} | \Delta | \phi_{h,lj} \rangle^2} & (\epsilon = E + \lambda \leq 0) \\ \sqrt{(E_h^0)^2 + \langle \phi_{h,lj} | \Delta | \phi_{h,lj} \rangle^2} + F_{lj}^{(h)}(E) - i\Gamma_{lj}^{(h)}(E)/2 & (\epsilon = E + \lambda > 0) \end{cases} \quad (\text{B14})$$

and the pole of $K_{lj}^{(1)}$, $E_n^{(1)}$ is

$$E_n^{(1)} \approx \sqrt{(E_h^0)^2 + \langle \phi_{h,lj} | \Delta | \phi_{h,lj} \rangle^2} + F_{lj}^{(h)}(E) \quad (\text{for } \epsilon = E + \lambda > 0) \quad (\text{B15})$$

approximately by supposing the pairing is weak and the energy dependence of $F_{lj}^{(h)}$ and $\Gamma_{lj}^{(h)}$ is small.

If E_h^0 exists above $-\lambda$ ($E_h^0 > -\lambda$), $E + E_h^0 > -2\lambda$ is satisfied when $\epsilon = E + \lambda > 0$. The second term of the denominator of Eq. (B7) is, therefore, negligible if $|\lambda|$ is large. Therefore $E_R^{(1)}$ and $E_n^{(1)}$ are given by

$$E_R^{(1)} \approx E_h^0 + F_{lj}^{(h)}(E) - i\Gamma_{lj}^{(h)}(E)/2, \quad (\text{B16})$$

$$E_n^{(1)} \approx E_h^0 + F_{lj}^{(h)}(E), \quad (\text{B17})$$

respectively. These are the same formulas, which were shown in Ref. [17].

2. Particle-type quasiparticle resonance

By supposing only one bound particle state in the system, Eq. (B5) is expressed as

$$S_{lj}^{(1)}(E) \approx \frac{E - E_p^0 - \frac{\langle \phi_{p,lj} | \Delta | \phi_{p,lj} \rangle^2}{E + E_p^0} - \frac{E - E_p^0}{E + E_p^0} W_{lj}^{(p)*}(E)}{E - E_p^0 - \frac{\langle \phi_{p,lj} | \Delta | \phi_{p,lj} \rangle^2}{E + E_p^0} - \frac{E - E_p^0}{E + E_p^0} W_{lj}^{(p)}(E)}, \quad (\text{B18})$$

where

$$W_{lj}^{(p)}(E) = F_{lj}^{(p)}(E) - i\Gamma_{lj}^{(p)}(E)/2 \quad (\text{B19})$$

$$F_{lj}^{(p)}(E) = \frac{2m}{\hbar^2} \frac{2}{\pi} P \int_0^\infty dk' k'^2 \frac{|\langle \psi_{0,lj}^{(+)}(k') | \Delta | \phi_{p,lj} \rangle|^2}{k_1^2(E) - k'^2}, \quad (\text{B20})$$

$$\Gamma_{lj}^{(p)}(E)/2 = \frac{2mk_1(E)}{\hbar^2} |\langle \psi_{0,lj}^{(+)}(k_1(E)) | \Delta | \phi_{p,lj} \rangle|^2, \quad (\text{B21})$$

$$E_p^0 = \epsilon_p - \lambda (> 0) \quad (\text{B22})$$

as the weak pairing approximation.

By using Eq. (B18), $T_{lj}^{(1)}(E)$ and $K_{lj}^{(1)}(E)$ are given by

$$T_{lj}^{(1)}(E) = \frac{\left(\frac{E - E_p^0}{E + E_p^0}\right) \Gamma_{lj}^{(p)}(E)/2}{E - E_p^0 - \frac{\langle \phi_{p,lj} | \Delta | \phi_{p,lj} \rangle^2}{(E + E_p^0)} - \left(\frac{E - E_p^0}{E + E_p^0}\right) W_{lj}^{(p)}(E)}, \quad (\text{B23})$$

$$K_{lj}^{(1)}(E) = \frac{\left(\frac{E - E_p^0}{E + E_p^0}\right) \Gamma_{lj}^{(p)}(E)/2}{(E - E_p^0) - \frac{\langle \phi_{p,lj} | \Delta | \phi_{p,lj} \rangle^2}{(E + E_p^0)} - \left(\frac{E - E_p^0}{E + E_p^0}\right) F_{lj}^{(p)}(E)}. \quad (\text{B24})$$

From Eqs. (B18) and (B24), the $S_{lj}^{(1)}$ pole $E_R^{(1)}$ and the $K_{lj}^{(1)}$ pole $E_n^{(1)}$ are given by

$$E_R^{(1)} \approx \begin{cases} \sqrt{(E_p^0)^2 + \langle \phi_{p,lj} | \Delta | \phi_{p,lj} \rangle^2} & (\epsilon = E + \lambda \leq 0) \\ \sqrt{(E_p^0)^2 + \langle \phi_{p,lj} | \Delta | \phi_{p,lj} \rangle^2} + \delta E_p W_{lj}^{(p)}(E) & (\epsilon = E + \lambda > 0) \end{cases} \quad (\text{B25})$$

and

$$E_n^{(1)} \approx \sqrt{(E_p^0)^2 + \langle \phi_{p,lj} | \Delta | \phi_{p,lj} \rangle^2} + \delta E_p F_{lj}^{(p)}(E) \quad (\text{for } \epsilon = E + \lambda > 0), \quad (\text{B26})$$

where δE_p is defined by

$$\delta E_p \equiv \frac{1}{2} \left(1 - \frac{E_p^0}{\sqrt{(E_p^0)^2 + \langle \phi_{p,lj} | \Delta | \phi_{p,lj} \rangle^2}} \right). \quad (\text{B27})$$

Note that δE_p is a very small value when the pairing is weak, therefore, the second term of Eqs. (B25) and (B26) can be neglected.

-
- [1] A. M. Lane and R. G. Thomas, *Rev. Mod. Phys.* **30**, 257 (1958).
[2] P. L. Kapur and R. E. Peierls, *Proc. Roy. Soc. A* **166**, 277 (1938).
[3] W. P. Wigner and L. Eisenbud, *Phys. Rev.* **72**, 29 (1947).
[4] H. Feshbach, *Ann. Phys. (NY)* **5**, 357 (1958).
[5] K. Mizuyama and Kazuyuki Ogata, *Phys. Rev. C* **86**, 041603(R) (2012).
[6] R. Jost and A. Pais, *Phys. Rev.* **82**, 840 (1951).
[7] K. Mizuyama, N. N. Le, T. D. Thuy, and T. V. Nhan Hao, *Phys. Rev. C* **99**, 054607 (2019).
[8] W. Horiuchi and Y. Suzuki, *Phys. Rev. C* **74**, 034311 (2006).
[9] H. Masui, W. Horiuchi, and M. Kimura, *Phys. Rev. C* **101**, 041303(R) (2020).
[10] M. Matsuo, K. Mizuyama, and Y. Serizawa, *Phys. Rev. C* **71**, 064326 (2005).
[11] K. Bennaceur, J. Dobaczewski, and M. Ploszajczak, *Phys. Lett. B* **496**, 154 (2000).
[12] M. Yamagami, *Eur. Phys. J. A* **25**, 569 (2005).
[13] K. Hagino and H. Sagawa, *Phys. Rev. C* **84**, 011303(R) (2011).
[14] N. Hinohara and W. Nazarewicz, *Phys. Rev. Lett* **116**, 152502 (2016).

- [15] G. Potel, A. Idini, F. Barranco, E. Vigezzi, and R. A. Broglia, *Rep. Prog. Phys.* **76**, 106301 (2013).
- [16] Y. Kobayashi and M. Matsuo, *Prog. Theor. Exp. Phys.* **2020**, 013D03 (2020).
- [17] K. Mizuyama, N. N. Le, and T. V. Nhan Hao, *Phys. Rev. C* **101**, 034601 (2020).
- [18] Amos de Shalit and Herman Feshbach, *Theoretical Nuclear Physics: Nuclear structure* (John Wiley & Sons, New York, 1974), p. 87.
- [19] R. G. Newton, *Inverse Schrodinger Scattering in Three Dimensions* (Springer, Berlin, 1989).
- [20] L. S. Rodberg and R. M. Thaler, *Introduction to the Quantum Theory of Scattering* (Academic Press, New York, 1967).
- [21] S. Aoyama, T. Myo, K. Kato, and K. Ikeda, *Prog. Theor. Phys.* **116**, 1 (2006).
- [22] T. Sasakawa, H. Okuno, S. Ishikawa, and T. Sawada, *Phys. Rev. C* **26**, 42 (1982); T. Sasakawa, *ibid.* **28**, 439 (1983); *Scattering theory* (Shokabo, Tokyo, 1991).
- [23] G. B. Arfken, H. J. Weber, and F. E. Harris, *Mathematical Methods for Physicists* (Academic Press, New York, 2011).
- [24] J. Mercer, *Philos. Trans. R. Soc., A* **209**, 415 (1909).